

# Investigation of electrical stimulation on phenotypic vascular smooth muscle cells differentiation in tissue-engineered small-diameter vascular graft

Sara Derhambakhsh <sup>a</sup>, Javad Mohammadi <sup>a,\*</sup>, Mohammad Ali Shokrgozar <sup>b</sup>, Hodjattallah Rabbani <sup>c</sup>, Niloufar Sadeghi <sup>c</sup>, Houra Nekounam <sup>d</sup>, Sotoudeh Mohammadi <sup>e</sup>, Ki-Bum Lee <sup>f</sup>, Mehrdad Khakbiz <sup>a,\*</sup>

<sup>a</sup> Division of Biomedical Engineering, Department of Life Science, Faculty of New Sciences and Technologies, University of Tehran, Tehran 439957131, Iran

<sup>b</sup> National Cell Bank of Iran, Pasteur Institute of Iran, Tehran, Iran

<sup>c</sup> Monoclonal Antibody Research Center, Avicenna Research Institute, ACECR, Tehran, Iran

<sup>d</sup> Department of Medical Nanotechnology, School of Advanced Technologies in Medicine, Tehran University of Medical Science, Tehran, Iran

<sup>e</sup> School of Medicine, Shahid Beheshti University of Medical Sciences, Tehran, Iran

<sup>f</sup> Department of Chemistry and Chemical Biology Rutgers, The State University of New Jersey, Piscataway, NJ 08854, USA

## ARTICLE INFO

### Keywords:

Cell migration  
Decellularized scaffold  
Electrical stimulation  
Phenotype change  
Tissue engineering  
Vascular smooth muscle cells

## ABSTRACT

In the development of vascular tissue engineering, particularly in the case of small diameter vessels, one of the key obstacles is the blockage of these veins once they enter the *in vivo* environment. One of the contributing factors to this problem is the aberrant proliferation and migration of vascular smooth muscle cells (VSMCs) from the media layer of the artery to the interior of the channel. Two distinct phenotypes have been identified for smooth muscle cells, namely synthetic and contractile. Since the synthetic phenotype plays an essential role in the unusual growth and migration, the aim of this study was to convert the synthetic phenotype into the contractile one, which is a solution to prevent the abnormal growth of VSMCs. To achieve this goal, these cells were subjected to electrical signals, using a 1000 µA sinusoidal stimulation at 10 Hz for four days, with 20 min duration per 24 h. The morphological transformations and changes in the expression of vimentin, nestin, and β-actin proteins were then studied using ICC and flow cytometry assays. Also, the expression of VSMC specific markers such as smooth muscle myosin heavy chain (SMMHC) and smooth muscle alpha-actin (α-SMA) were evaluated using RT-PCR test. In the final phase of this study, the sheep decellularized vessel was employed as a scaffold for seeding these cells. Based on the results, electrical stimulation resulted in some morphological alterations in VSMCs. Furthermore, the observed reductions in the expression levels of vimentin, nestin and β-actin proteins and increase in the expression of SMMHC and α-SMA markers showed that it is possible to convert the synthetic phenotype to the contractile one using the studied regime of electrical stimulation. Finally, it can be concluded that electrical stimulation can significantly affect the phenotype of VSMCs, as demonstrated in this study.

## 1. Introduction

Cardiovascular diseases, such as atherosclerosis and coronary arterial restenosis, are among the leading causes of death (Catto et al., 2014). The most prevalent treatment procedures in the early stages of illness are angioplasty and stenting. Bypass surgery is required when a

patient has substantial coronary artery blockage (Isenberg et al., 2006). A fundamental issue with autologous graft transplantation is the lack of a suitable vein or artery in the patient's body (Trueta and Harrison, 1953). Vascular tissue engineering, as a potentially promising method, has made it possible to generate vascular constructs with mechanical and biological properties similar to those of native vessels, eliminating

**Abbreviations:** VSMCs, vascular smooth muscle cells; SMMHC, smooth muscle myosin heavy chain; α-SMA, smooth muscle alpha-actin; ICC, Immunocytochemistry; H&E, Hematoxylin-eosin staining; SEM, Scanning Electron Microscopy.

\* Corresponding authors.

E-mail addresses: [Javad.Mohammadi@ut.ac.ir](mailto:Javad.Mohammadi@ut.ac.ir) (J. Mohammadi), [khakbiz@ut.ac.ir](mailto:khakbiz@ut.ac.ir) (M. Khakbiz).

<https://doi.org/10.1016/j.tice.2022.101996>

Received 18 July 2022; Received in revised form 4 December 2022; Accepted 5 December 2022

Available online 13 December 2022

0040-8166/© 2022 Elsevier Ltd. All rights reserved.

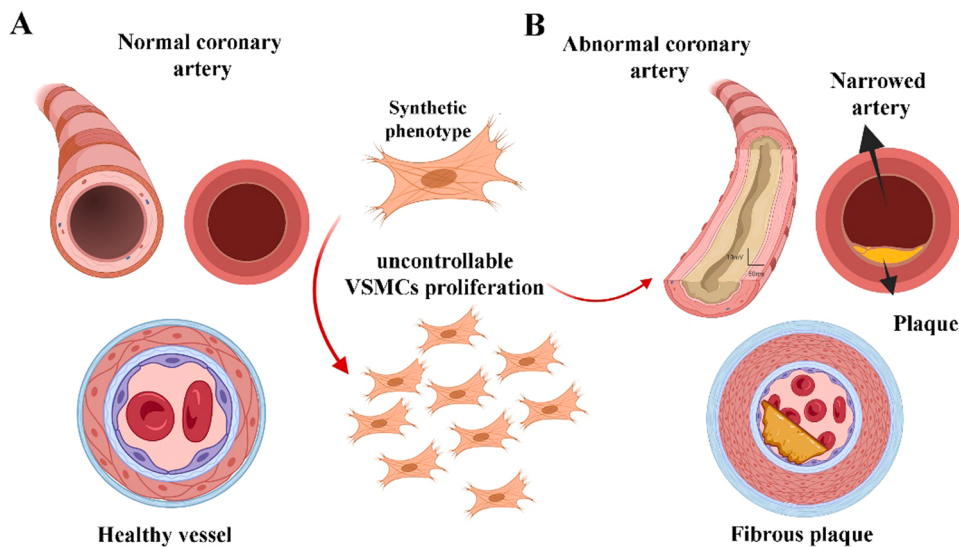


**Fig. 1.** (A) a normal coronary artery (B) an abnormal coronary artery (Created by BioRender).

the limitations of autologous and synthetic grafting methods (Williams and Wick, 2005).

Each vessel is made up of three layers including intima, media, and adventitia. The media layer contains vascular smooth muscle cells (VSMCs), which play key roles not only in blood vessel physiological processes such as vasoconstriction, vasodilation, and extracellular matrix formation but also in the etiology of vascular disorders such as atherosclerosis and hypertension (Bacakova et al., 2018a; Lacolley et al., 2012; Shi et al., 2020). Many investigations have been conducted on the mechanisms related to the proliferation, migration, and phenotypic differentiation of these cells (Gerthoffer, 2007; Louis and Zahradka, 2010; Jensen et al., 2021; Ilanlou et al., 17, 2019). One of the most difficult issues in vascular tissue engineering is to inhibit the aberrant proliferation and migration of VSMCs from the media layer to the intima and vessel lumen, which results in vessel closure and graft rejection (Kloc and Ghobrial, 2014; Ilanlou et al., 2019).

VSMCs have two distinct phenotypes, namely synthetic and contractile (Bacakova et al., 2018a; Rensen et al., 2007). The synthetic type of VSMCs plays an essential role in the aberrant proliferation and migration of these cells (Owens et al., 2004; Zhang et al., 2020). The cellular population of the synthetic phenotype increases after VSMCs isolation and numerous cell culturing and passaging assays (Rzucidlo et al., 2007). Increased synthetic phenotype results in the uncontrollable VSMCs proliferation and subsequent blockage of small diameter vessels (Fig. 1). Controlling the proliferative activity of VSMCs and inducing them toward a contractile phenotype is essential in vascular tissue engineering (Bacakova et al., 2018b). In the *in vivo* environment, many factors related to endothelial cells can affect VSMCs proliferation. For example, endothelial cells express PDGF and bFGF, which can promote VSMCs proliferation (Grosskreutz et al., 1999), while expression of inhibitors such as heparin & TGF $\beta$  by these cells can prevent the proliferation of VSMCs (Scott-Burden and Vanhoutte, 1994). On the other hand, many factors can affect the differentiation of VSMCs (Saleh Al-Shehabi et al., 2016) see in Fig. (S-1) (supplementary file).

Various studies have been conducted on the effects of different agents such as growth factors, serum, nitric oxide (NO), mechanical and electrical stimulations, etc. on the performance of VSMCs, such as differentiation and proliferation. For example, a long-term culture using a high serum content and increased levels of PDGF-BB and TGF $\beta$ 1 can induce the synthetic VSMCs phenotype, while serum starvation and deprivation of PDGF-BB can promote the contractile VSMCs phenotype (Wanjare et al., 2013). In a study on the impact of NO, released from liposomes, on preventing intimal hyperplasia, it has been concluded that

an optimized NO congestion can prevent the phenotype conversion of VSMCs from contractile to synthetic and the subsequent migration and intimal hyperplasia (Huang et al., 2009). The impact of electrical stimulation on VSMCs has been the subject of various studies. For instance, in a research on the effect of this stimulation on intimal hyperplasia, it was demonstrated that electrical stimulation could inhibit VSMCs proliferation, thereby preventing intimal hyperplasia (Zhang et al., 2010). In another investigation, application of a continuous and constant 50  $\mu$ A (0.6 V) sinusoidal electrical stimulation on VSMCs cultured on conducting polypyrrole (PPy) substrates coated with collagen IV, could direct synthetic VSMCs toward the contractile phenotype (Rowlands and Cooper-White, 2008).

Considering previous reports about the impacts of electrical cues on the performance of VSMCs, in this study, we have examined the effect of electrical stimulation on phenotype switching of VSMCs based on morphological changes and expression of vimentin, nestin,  $\beta$ -actin proteins, and VSMC differentiation markers including SMMHC and  $\alpha$ -SMA that are known as markers of the contractile phenotype (Beamish et al., 2010). Thereafter, VSMCs were cultured on the decellularized sheep vessel as a scaffold and subjected to electrical stimulation. Finally, scanning electron microscopy (SEM) analysis was carried out. Decellularization of the scaffold was done via a vessel bioreactor. This is the first work on the influence of electrical stimulation on the expression of vimentin, nestin, and  $\beta$ -actin proteins by VSMCs, and also on the morphology and proliferation of the VSMCs seeded on a decellularized scaffold.

Although the synthetic phenotype is necessary for remodeling of the injured vessels, it can be associated with uncontrolled proliferation in the engineered vascular tissues and also in many vascular diseases such as atherosclerosis, intimal hyperplasia, etc. Previous studies have shown that in these cases, the contractile phenotype of VSMCs can be converted to the synthetic phenotype. The migratory and proliferative properties of the synthetic phenotype can result in occlusion in vessels.

## 2. Materials and methods

### 2.1. Decellularization

The carotid artery was isolated from a sheep. After cleaning and separating fats and other excess tissues, the veins were rinsed with sterile water for 2 h, prior to dynamic and static decellularizations.

To perform dynamic decellularization, three thawing-freezing steps were first performed, such that in each step, the isolated vessels were



**Fig. 2.** Decellularization process using a vessel bioreactor.

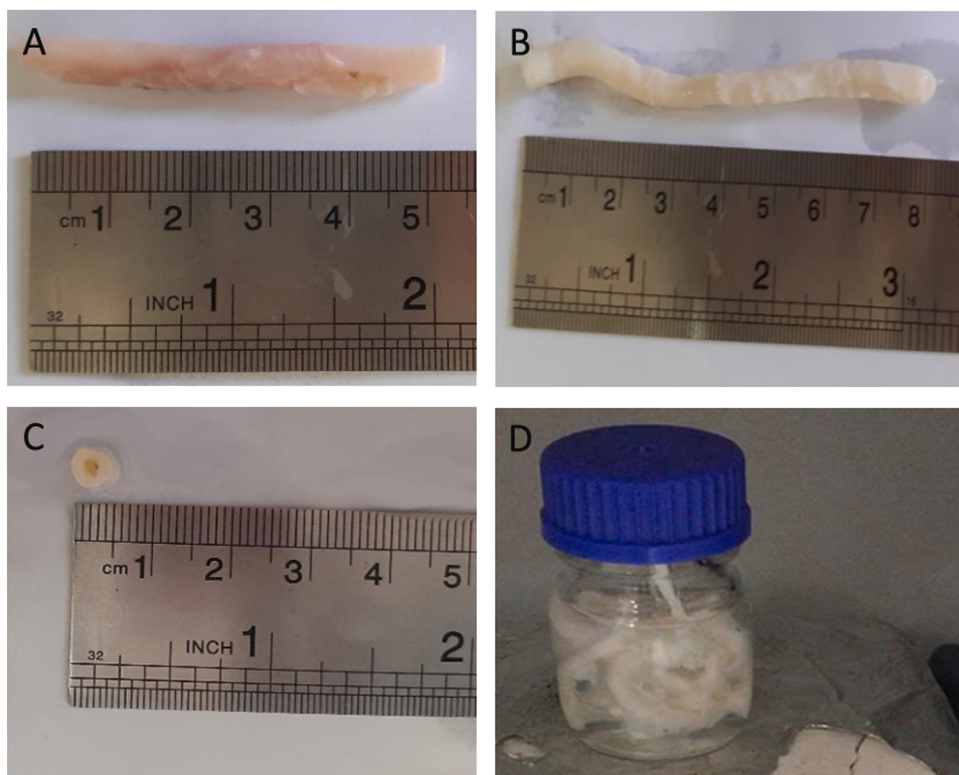


**Fig. 3.** Sheep's vessel. A) before decellularization B) after decellularization using a bioreactor; C) cross section of the decellularized vessel D) decellularized vascular graft by the static method.

**Table 1**  
Forward and reverse sequences of primers for MyHC1,  $\alpha$ -SMA, and GAPDH.

Name	Sequence	length	Tm	Amplicon
MyHC1 - F	TGGATGATCTACACCTACTC	20	59	141
MyHC1 - R	CAGAGATAGAGAAGATGTGG	20	59	
Actin-F	CTCTCTGTCTACCTTCAA	19	59	119
Actin-R	ATACTGTCGCTCTGAGTGTA	20	59	
GAPDH-F	CAGAACATCATCCCTGCATCC	21	59	119
GAPDH-R	ACAACGGATAACATTGGGGTA	21	59	

placed in a freezer at  $-80^{\circ}\text{C}$  for 2 h and then immersed in PBS 1X solution at room temperature. Thereafter, the scaffolds, being about 4 cm long, were transferred into a bioreactor chamber (Fig. 2). After connecting to the pump, they were placed in hypertonic solution (1.1 % NaCl and 0.02 % EDTA (Gibco, United States)) and then hypotonic solution (0.7 % NaCl and 0.02 % EDTA). Then, 0.05 % trypsin (Gibco, United States) and 0.02 % EDTA were added to the bioreactor chamber

for washing the inner and outer walls for 24 h. The samples were then exposed to 0.1 % NH4OH for 24 h and then placed in 1 % Triton-X-100 (Merk, Germany) for 48 h, while this solution was changed after 24 h. Finally, the scaffolds were rinsed in PBS 1X for 24 h, and added with penicillin-streptomycin (Gibco, United States) (0.2 mg/ml). Fig. 3(a, b, c) shows the sheep vessel before and after the decellularization process. To conduct static decellularization, the rinsed vessels were placed in NaCl (1.2 %) solution for 2 h at  $4^{\circ}\text{C}$  in the fridge. Thereafter, the vessels were transferred to PBS solution for 2 h. Then, they were exposed to Trypsin (0.25 %) for 24 h in the fridge. In the next step, vessels were rinsed with PBS 1X and then exposed to TritonX100 (1 %) for 48 h at  $4^{\circ}\text{C}$  in the fridge. Finally, the decellularized vessels were rinsed with PBS 1X and penicillin-streptomycin (0.2 mg/ml), as shown in Fig. 3. (d).

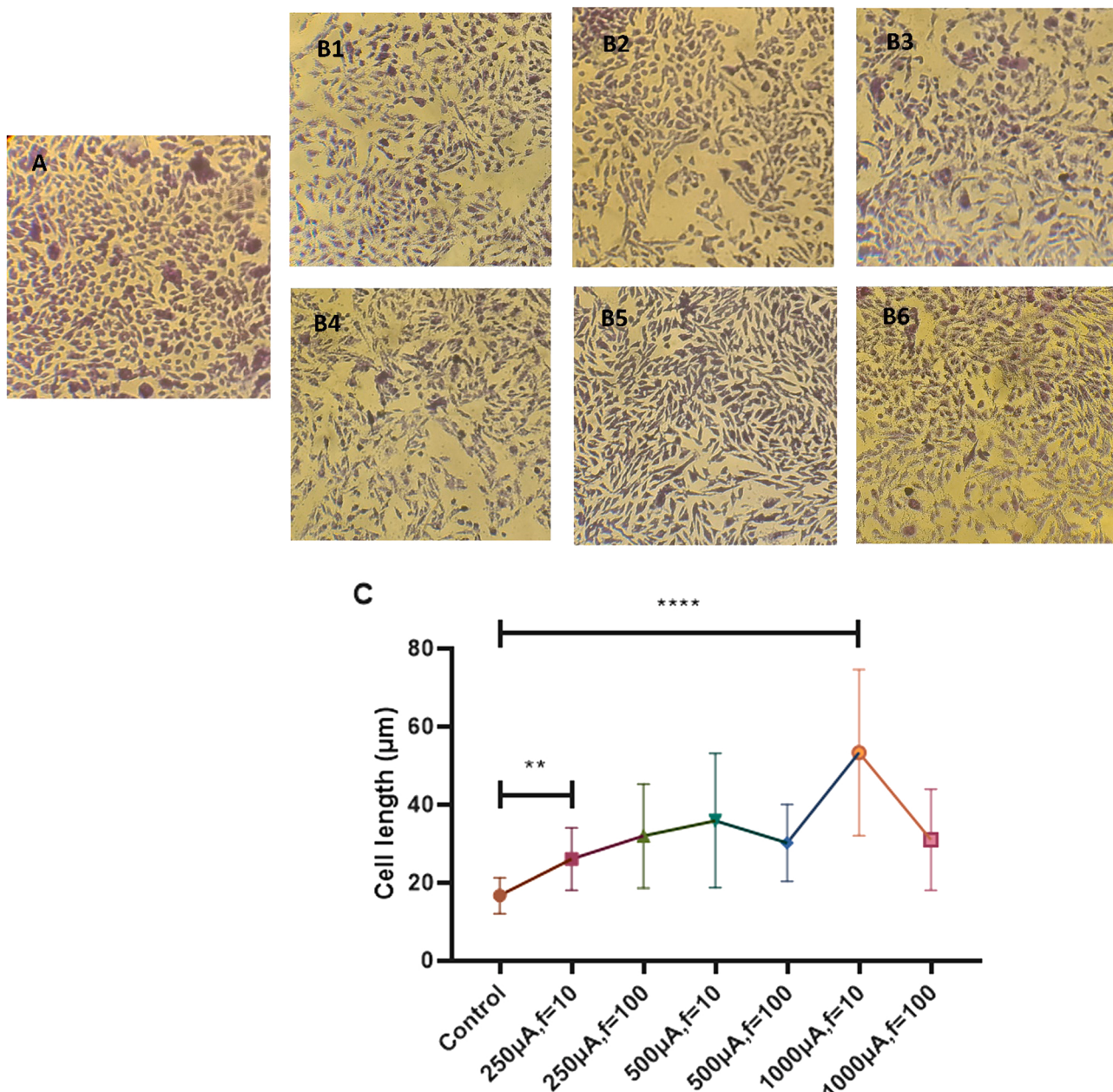


**Fig. 4.** Crystal violet stained non-stimulated and stimulated VSMCs after four days, using the following electrical stimulation amplitudes and frequencies (10X). (A) non-stimulated VSMCs after four days (Control); B) stimulated VSMCs after four days, (1) 250 µA, f = 10 Hz (2) 250 µA, f = 100 Hz, (3) 500 µA, f = 10 Hz, (4) 500 µA, f = 100 Hz, (5) 1000 µA, f = 10 Hz, (6) 1000 µA, f = 100 Hz, P < 0.0001: \*\*\*\*, P = 0.0075: \*\*; C) VSMCs length on the fourth day using the sinusoidal electrical stimulation.

## 2.2. Histology

### 2.2.1. Hematoxylin-eosin staining (H&E)

After the decellularization step, vessel specimens were prepared, processed in paraformaldehyde 4% in PBS, and then embedded in paraffin and cut with a microtome device. The resulting slices were stained with hematoxylin-eosin.

## 2.3. Cell culture

Vascular smooth muscle cell line (A-10) was obtained from the National Cell Bank of Iran, Pasteur Institute, Iran. These cells were cultured in 24-well cell culture plates and incubated with DMEM-F12 (Gibco, United States) supplemented with 10 % FBS. VSMCs at passages 2–6 were used for experiments.

For culturing the cells on the decellularized scaffold, the scaffold was first immersed in 70 % ethanol for about 30 min and then washed with PBS 1X three times under a sterile laminar flow hood at 15-minute intervals. Then the scaffold was exposed to UV for about an hour, and then penestrept was added to the solution containing the scaffold. The scaffold was washed several times with PBS 1X. At the end, VSMCs were seeded on the scaffold at a density of  $3 \times 10^5$  cells/cm<sup>2</sup> and incubated in a humidified atmosphere, with 5 % CO<sub>2</sub> for 72 h.

## 2.4. Electrical stimulation

In this research, a signal generator device (Victor 2015 H, China) was used to generate the electrical current. The voltage could be adjusted depending on the desired current in this device. An electrical resistor (1 K) was placed in the output current path of the device, and then 1000,

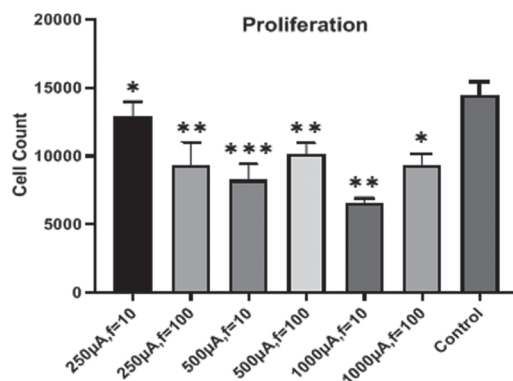


**Fig. 5.** Cell growth rates before and after electrical stimulation,  $P < 0.05$ : \*,  $P < 0.005$ : \*\*,  $P < 0.0005$ : \*\*\*.

500, and 250  $\mu$ A sinusoidal electrical stimulations at 10 Hz and 100 Hz were generated. At first, these electrical stimulations were applied to the cultured cells in a 24-well plate for four days, with 20 min duration per 24 h. After assessing cell differentiation and optimizing the proper electrical current for changing the phenotype, the 1000  $\mu$ A sinusoidal electrical stimulation at 10 Hz was selected and applied to the cells seeded on the decellularized scaffold using the mentioned time schedule. For electrical stimulation, set-up used (Nekounam et al., 2022) to transfer electrical current to the cultured cells in 24-well plate and scaffold, two sterile stainless-steel screws were inserted in each well so that electrical current entered each well from one screw and exited through the other one.

## 2.5. Immunofluorescence, protein analysis, gene expression, and cell imaging

### 2.5.1. Immunocytochemistry

Two groups of cells were cultured in a 24-well cell culture plate. One group was considered as the control and the other one was subjected to a 1000  $\mu$ A sinusoidal electrical stimulation at 10 Hz, for 20 min, every 24 h. After 72 h, cells were fixed with paraformaldehyde 4 % diluted with PBS 1X for 10 min at room temperature. Then, they were permeated with TritonX100, 0.1% diluted with PBS 1X for 15 min at room temperature. In the next step, cells were washed with PBS 1X twice. Thereafter, cell membranes were blocked in the sheep serum 5% for 15 min and then incubated with  $\beta$ -actin, vimentin, and nestin primary antibodies (Padzaco, Iran) for 1 h hour, separately, followed by washing with PBS 1X, twice. After these steps, cells were incubated with FITC-conjugated secondary antibody for 1 h and then rinsed with PBS 1X. Cell imaging was performed using an inverted microscope (Olympus, CKX-41, Germany) and a camera (Olympus, DP71, Germany). It is notable that in this experiment, all incubations were performed at room temperature.

### 2.5.2. Flow cytometry

Cells were transferred to the flow cytometry tubes (100,000 cells per tube), which included positive and negative controls of FITC and  $\beta$ -actin, vimentin, and nestin antibodies (Padzaco, Iran). Then, they were permeated with TritonX100, 0.1% diluted with PBS 1X for 15 min at room temperature. In the next step, cell membranes were blocked in the sheep serum 5 % for 15 min. After this step, primary antibodies were added to the corresponding tubes and incubated for 1 h. Then, cells were washed with TritonX100, 0.1 % and centrifuged at 1500 rpm and 5 min, twice. Afterwards, the cells were incubated with FITC-conjugated secondary antibody for 1 h followed by washing with TritonX100, 0.1% and centrifuging at 1500 rpm and 5 min twice. Finally, the prepared flow cytometry tubes containing the cells were used for analysis using a flow cytometry device (Becton Dickinson, USA) and FlowJo 7.6

software.

### 2.5.3. RNA extraction and real-time quantitative PCR (qRT-PCR)

Total RNA of VSMCs samples were extracted by Ribogreen kit (GeneAll, Korea) according to manufacturer instruction. The quality and quantity of extracted RNA were checked with 1 % agarose gel electrophoresis and Nanodrop (Thermo Scientific NanoDrop 2000c), respectively. 3  $\mu$ g of RNA was treated with 1  $\mu$ l DNase I (Thermo Scientific, USA), 1  $\mu$ l 10X buffer and incubation in 37 °C for 30 min follow by reaction termination with 1  $\mu$ l EDTA 50 mM. complementary DNA (cDNA) was synthesized based on ExcelRT Reverse transcription kit (SMOBIO) including 1  $\mu$ g RNA, 1  $\mu$ l oligo(dT) primer and 1  $\mu$ l dNTPs incubated in 70 °C for 10 min. After that, cDNA synthesis completed with 1  $\mu$ l Reverse transcriptase, 1  $\mu$ l RNase inhibitor and 4  $\mu$ l 5× buffer incubated in 42 °C for 60 min. Furthermore, primer design for each target gene was determined based on primer3 in Geneious IR9.1.8 software, considering the optimal melting temperature between 58 and 60 degrees. The forward and reverse sequences of primers for target genes, including smooth muscle myosin heavy chain (MyHC1; NM\_001135158.1), smooth muscle alpha-actin ( $\alpha$ -SMA; NM\_019183.1), and Glyceraldehyde 3-phosphate dehydrogenase (GAPDH; NM\_017008.4) as endogenous control gene (Table 1). The real-time quantitative PCR (Rotor gene Real-Time PCR, Qiagene) was accomplished with reaction of 20  $\mu$ l containing 10  $\mu$ l SYBR green kit (Ampliqon SYBR green 2x), 0.2  $\mu$ M each primer and 1  $\mu$ l cDNA with thermal program: Holding stage at 95 °C for 10 minutes followed by 40 cycles of 94 °C for 15 s, 59 °C for 20 s and 72 °C for 30 s. All samples analyzed in triplicate reactions with melt curve assay of reactions between 65 °C and 95 °C. Realtime mRNA fold change of target genes was calculated based on  $2^{-\Delta\Delta CT}$  formulae (Livak and Schmittgen, 2001) with normalization of Ct values in relative of control samples and endogenous GAPDH gene.

### 2.5.4. Scanning electron microscopy

After culturing the cells on the scaffold and electrical stimulation, the constructs were fixed in Paraformaldehyde 4 % and washed with 30 %, 50 %, 75 %, and 95 % ethanol, respectively. At the end, the cells were imaged using a scanning electron microscope (MIRA3 TESCAN, Czech).

### 2.5.5. Statistical analysis

In this research, GraphPad Prism 7 software was used for statistical analysis. Data comparison was performed using the one-way ANOVA method between multiple groups and the t-test method between two groups. P values less than 0.05 were assumed to be statistically significant.

## 3. Results and discussion

### 3.1. Cell morphological changes before and after electrical stimulation

After applying 1000, 500, and 250  $\mu$ A sinusoidal electrical stimulation at 10 Hz and 100 Hz to VSMCs, their morphological changes were monitored every 24 h under a microscope. The greatest morphological changes were observed on the fourth day using the 1000  $\mu$ A sinusoidal electrical stimulation at 10 Hz (Fig. 4). On the other hand, the number of cells was counted in these 6 groups after four days of electrical stimulation through Neobar lam. As can be seen in Fig. 5, the results were significantly different from those of the control group. Meanwhile, the smallest growth was achieved after 1000  $\mu$ A and 10 Hz stimulation, as shown in Fig. 5.

As the contractile phenotype has elongated morphology and lower proliferation compared to the synthetic phenotype of VSMCs (Chakraborty et al., 2021), this morphological change and the smallest growth may indicate a change in phenotype due to electrical stimulation. The effect of electrical stimulation on the expression of vimentin, nestin,  $\beta$ -actin proteins and VSMCs differentiation markers such as SMMHC and  $\alpha$ -SMA were investigated to determine the phenotype of VSMCs (Fig. 6).

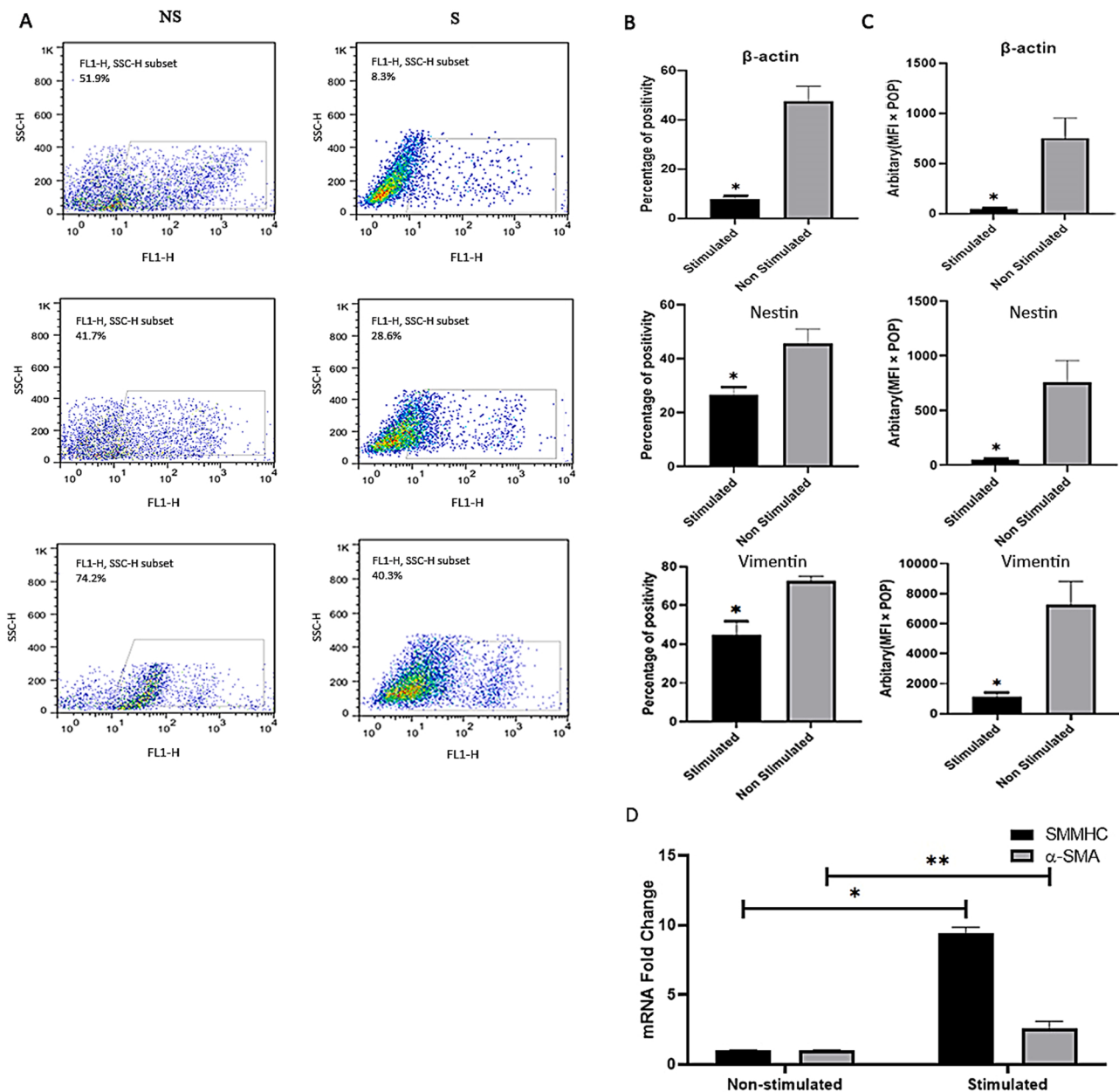


**Fig. 6.** A) Flow cytometry results of  $\beta$ -actin, nestin, and vimentin proteins before and after electrical stimulation, Left panel: A) Non-stimulated VSMCs compared to 1000  $\mu$ A, 10 Hz sinusoidal AC stimulated VSMCs B) The same results illustrated as bars for better visualization. Right panel: C) The average FITC intensities were calculated by multiplying the mean fluorescence intensity by the percentage of positivity ( $MFI \times POP$ ); D) Significant increase in the relative expression of SMMHC and  $\alpha$ -SMA m-RNA by stimulated VSMCs compared to non-stimulated cells.  $P < 0.05$ : \*,  $P < 0.005$ : \*\*.

It can be seen that the maximum difference in cell content between the control and experimental samples is obtained after the 1000  $\mu$ A and 10 Hz stimulation.

### 3.2. Investigation of vimentin, nestin and $\beta$ -actin proteins and SMMHC and $\alpha$ -SMA m-RNA levels

Beta-actin is one of the six different isoforms of actin. This protein, one of the two non-muscle cytoskeletal actins, has been mainly found near dense bodies and longitudinal channels, among other places (Yamin and Morgan, 2012). While both phenotypes of VSMCs express  $\beta$ -actin, their expression levels for this protein are different, such that  $\beta$ -actin expression level by the synthetic phenotype is substantially higher than that of contractile phenotype. According to a previous study on the expression of structural proteins by the two VSMC phenotypes

using western blot analysis, the expression levels of several proteins were similar between the two phenotypes, but in the case of some proteins, including  $\beta$ -actin, there were different expressions, such that the expression level of  $\beta$ -actin by the synthetic phenotype was significantly more than that by the contractile phenotype (Worth et al., 2001). In this research,  $\beta$ -actin expression, measured by flow cytometry test, decreased after a 1000  $\mu$ A sinusoidal electrical stimulation at 10 Hz by approximately 43 % (from 51.9 % to 8.34 %) (Fig. 6).

Nestin is expressed in stem cells, nerve cells, and muscle cells. Intermediate filaments are critical players in polarity maintenance in migrating cells (Leduc and Etienne-Manneville, 2015, 2017; Seetharaman and Etienne-Manneville, 2020). Evidence suggests that following malignancy, nestin helps to improve the ability of cancer cells to migrate and metastasize (Chung et al., 2013). Nestin exists in VSMCs and directly contributes to cell proliferation (Tardif et al., 2014). The

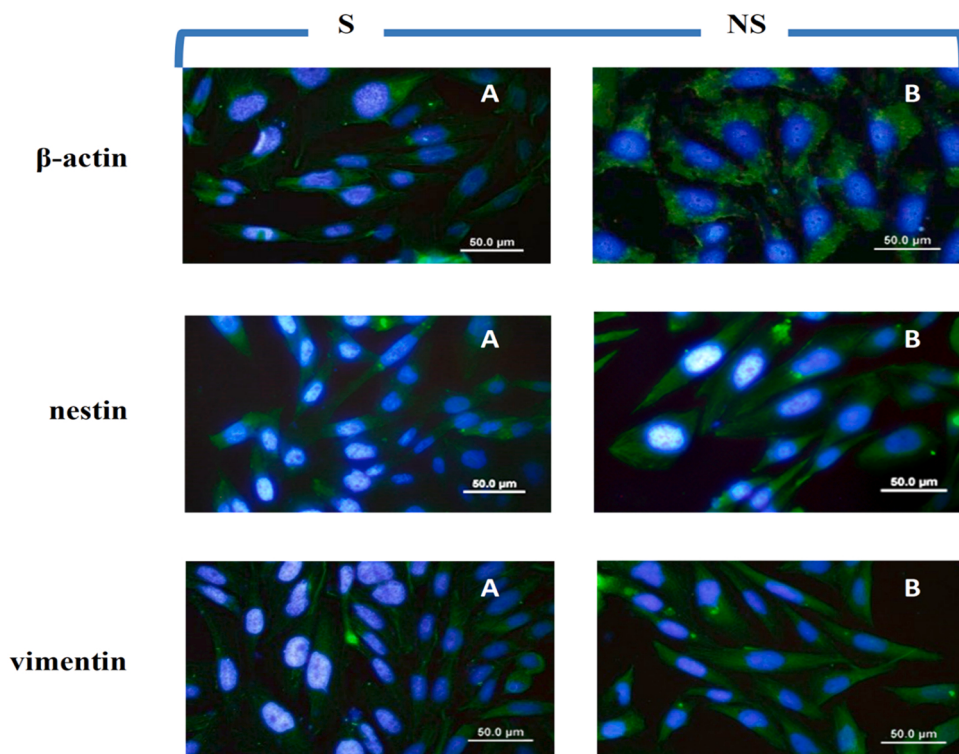


**Fig. 7.** The expression of  $\beta$ -actin, Nestin, and Vimentin proteins with antibody conjugated to FITC , A) 1000  $\mu$ A, 10 Hz sinusoidal AC stimulated VSMCs. B) Non-stimulated VSMCs.

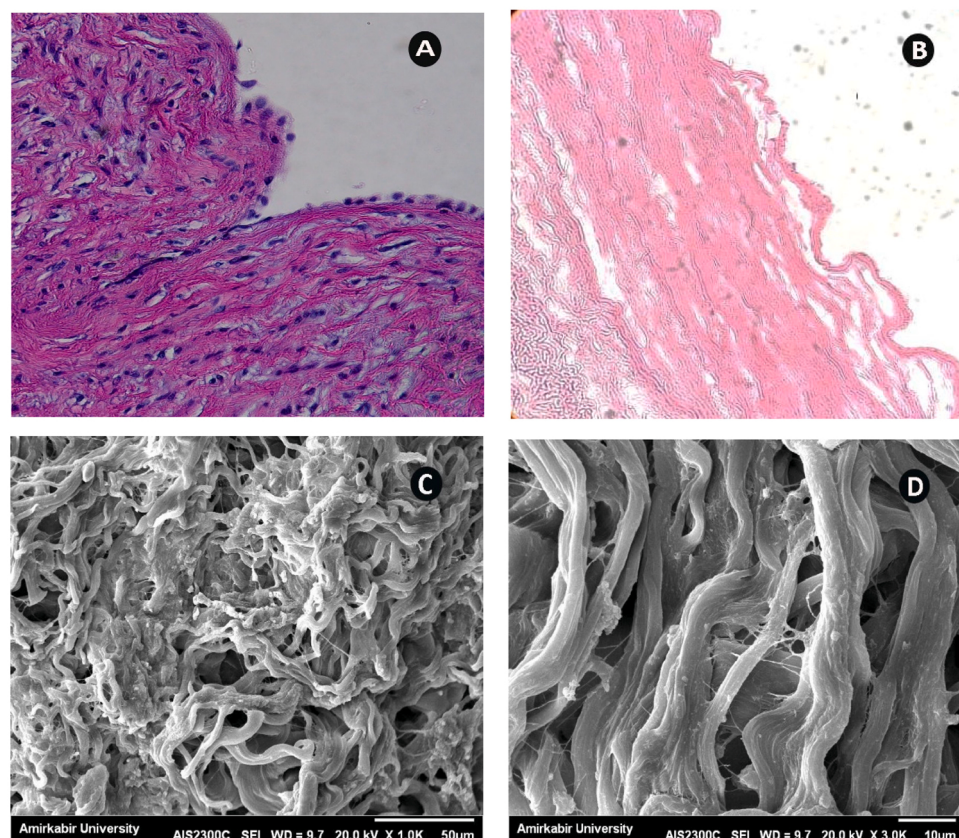


**Fig. 8.** Carotid artery of sheep A) before decellularization; B) after decellularization, such that a cell-free extracellular matrix was observed; C) SEM image of ECM structure after decellularization (low magnification) the filament median size:4  $\mu$ m; and D) SEM image of ECM structure after decellularization (high magnification).

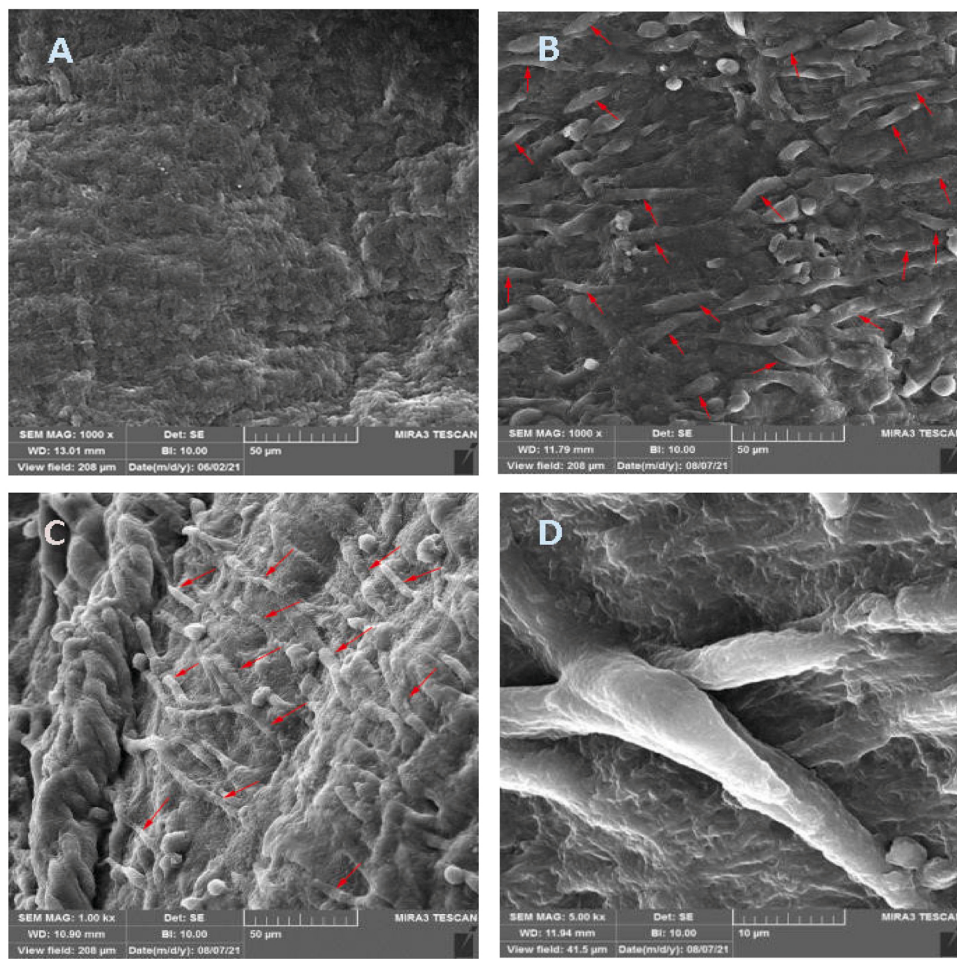


**Fig. 9.** (A) carotid artery after decellularization; (B) non-stimulated VSMCs cultured on the scaffold after 72 h, red arrows indicate examples of non-stimulated VSMCs cultured on the decellularized scaffold; (C) 1000  $\mu$ A, 10 Hz sinusoidal electrical stimulated VSMCs cultured on the decellularized scaffold, red arrows indicate examples of stimulated VSMCs; (D) stimulated cell in high magnification.

**Table 2**

The length of stimulated and non-stimulated vascular smooth muscle cells.

Cell type	Cell length range (Micrometers)	Cell length average (Micrometers)	Standard deviation	median value (Micrometers)
Non-Stimulated	10.07–50.78	27.05	9.69	26.116
Stimulated	25.26–67.16	47.386	13.051	48.001

amount of this protein is increased during damage and remodeling of VSMCs (Oikawa et al., 2010). Since the synthetic phenotype of VSMCs has an essential role in cell migration, proliferation, and remodeling (Bacakova et al., 2018a; Rzucidlo et al., 2007; Hu et al., 2019), nestin expression should be higher in the synthetic phenotype, compared to the contractile phenotype. In this research, nestin expression after electrical stimulation decreased by around 15% (Fig. 6).

Vimentin is a major intermediate filament protein in the vascular smooth muscle cell and airways (Halayko et al., 1996; Johansson et al., 1997; Tang et al., 2005). Vimentin intermediate strands attach to desmosomes (intercellular junctions) on the membranes and dense bodies in the cytoplasm, and create a structural basis for the transition of intercellular and intracellular forces in smooth muscle. A greater amount of vimentin filaments is present in VSMCs, compared to other smooth muscles such as those existing in the respiratory, digestive, and urogenital smooth muscles. This difference can be indicative of a different differentiation pathway for VSMCs, in comparison with other types of smooth muscle cells and may be relevant to the special functions and pathological conditions of the blood vessels (Gabbiani et al., 1981).

**Fig. (S-2)** (supplementary file), shows the location of the Vimentin proteins (Battaglia et al., 2018).

A previous research has revealed that vascular wall softening due to ECM-degradation and improper collagen cross-linking in pathological conditions could increase switching to synthetic phenotype and the expression of related genes such as vimentin (Shao et al., 2020). According to another study on comparing vimentin expression between the two VSMC phenotypes, the amount of vimentin expression in the synthetic phenotype is higher than that in the contractile type (Worth et al., 2001). Another research revealed that the vimentin expression decreases during the differentiation of synthetic phenotype to the contractile one (van der Loop et al., 1997). Vimentin filaments are involved in cell migration (Battaglia et al., 2018; Tang et al., 2019; Li et al., 2006) and motility (Mendez et al., 2010; Dmello et al., 2016). Since cell migration is one of the functions and characteristics of the synthetic phenotype, it can be deduced that vimentin expression in the synthetic phenotype is higher than that in the contractile phenotype.

In this research, the amount of vimentin was estimated by flow cytometry. According to these results, vimentin expression after

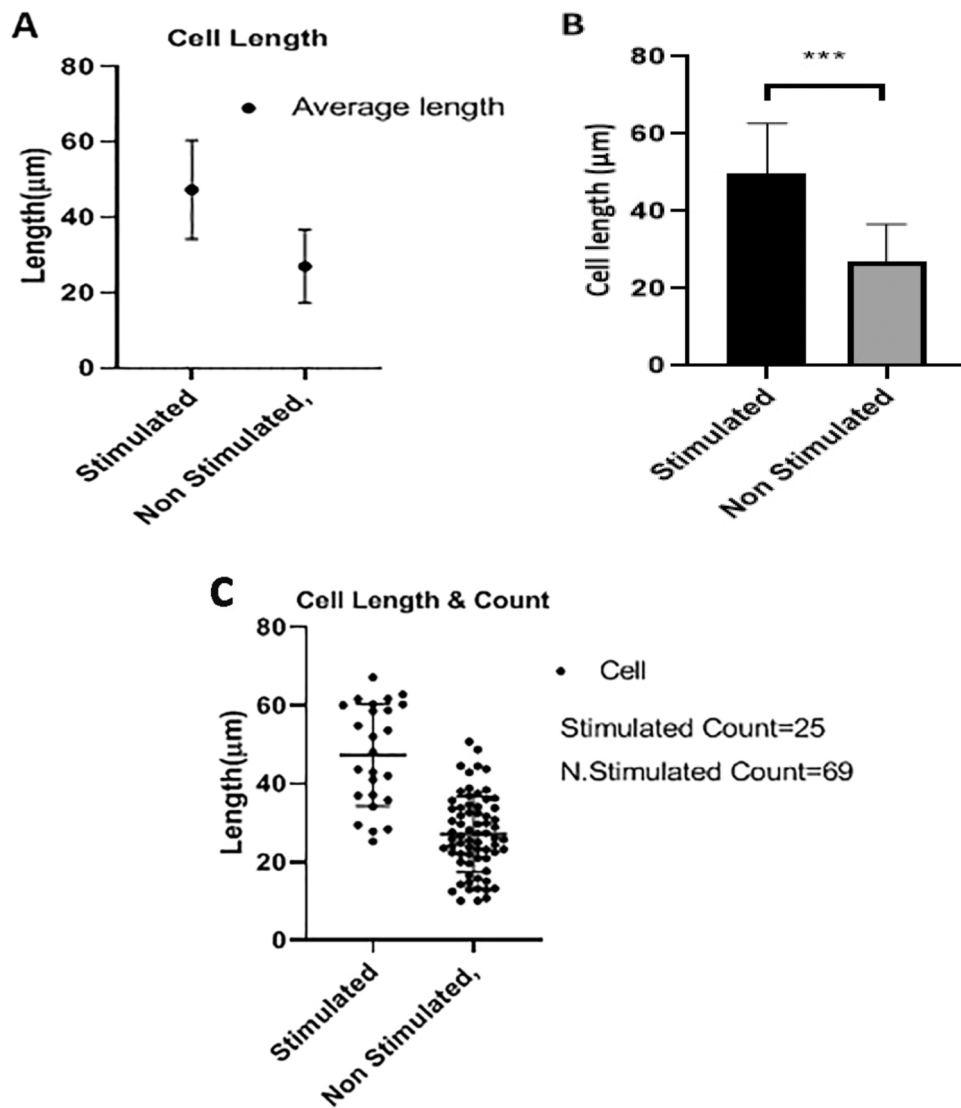


**Fig. 10.** A, B) Cell lengths of stimulated and non-stimulated VSMCs,  $P < 0.0005$ : \*\*\*; C) Cell lengths and counts of stimulated and non-stimulated VSMCs (calculated using the ImageJ software).

applying a 1000  $\mu$ A sinusoidal electrical stimulation at 10 Hz decreased by around 30 % (Fig. 6).

Immunocytochemistry (ICC) was also utilized to examine the expression of beta-actin, nestin, and vimentin. Similar results were seen in immunofluorescent images taken at the same time points. These tests were done before and after applying the 1000  $\mu$ A and 10 Hz sinusoidal electrical stimulation (Fig. 7).

The contractile and synthetic types of VSMCs express different levels of related markers. Smooth muscle contraction-related proteins such as  $\alpha$ -SMA and SMMHC are expressed at reduced quantities by synthetic VSMCs (Petsophonsakul et al., 2019). SMMHC is the particular marker protein that best defines a mature contractile SMC phenotype (Rensen et al., 2007). Additionally,  $\alpha$ -SMA is a marker for the contractile phenotype of SMCs and prevents migration and proliferation of VSMCs by inhibiting Rac1 activity (Chen et al., 2016). In this research, the expression levels of VSMC differentiation markers including SMMHC and  $\alpha$ -SMA were investigated. According to the obtained results, the expression level of these markers significantly increased after electrical stimulation (Fig. 6d).

Based on the obtained result, electrical stimulation can change the expression levels of the studied proteins and consequently, can direct the phenotype of VSMCs from the synthetic to the contractile type. Although

the mechanisms behind the changes in the expressions of vimentin, nestin, and  $\beta$ -actin proteins through electrical stimulation is not exactly known, phenotype switching in response to electrical stimulation can be interceded by the changes in the amount of  $\text{Ca}^+$ . The voltage-dependent sodium and calcium channels, which are closed during cell rest, open when voltage is applied, and consequently the sodium and calcium ions enter the cell, and the inside potential of the membrane becomes positive, and finally these channels are closed again.  $\text{Ca}^+$  can have activation as a secondary messenger in the reaction of electrical stimulation that affects the migration, proliferation, and contraction of VSMCs (House et al., 2008). For example, electrical stimulation through depolarization can increase  $\text{Ca}^+$  concentration and consequently upregulate the differentiation pathway. Then, the expression of differentiation marker proteins such as SMMHC and  $\alpha$ -SMA through regulation of the RhoA/ROK/myocardin pathway increases (Wamhoff et al., 2004). Moreover, after stimulation, the increase in intracellular calcium creates a binding site between the myosin light chain (MLC) filaments and contractile actins such as  $\alpha$ -actin. It can lead to the activation of the contractile apparatus (Kuo and Ehrlich, 2015; Amberg and Navedo, 2013) see in Fig. (S-3) (supplementary file). This can be probably a factor for inducing differentiation to the contractile phenotype via electrical stimulation.

It has been reported that electrical stimulation can affect the proliferation of VSMCs and increase the expression of p27Kip1 and PTEN genes (Zhang et al., 2010). Cell proliferation can be adjusted by various factors such as p27Kip1 and PTEN. P27Kip1 is a broad-spectrum, cyclin-related kinase suppressor that has an essential role in regulating the cell cycle and can prevent cell proliferation (Coats et al., 1996). Increasing p27Kip1 can decrease neointimal thickness in a balloon-injured artery model (Ueno et al., 1997). The high proliferative ability is one of the synthetic phenotype characteristics and applying electrical stimulation can contribute to reducing cell proliferation. Overall, it can be concluded that electrical stimulation can induce phenotype differentiation from the synthetic phenotype to the contractile.

### 3.3. Decellularization and cell culture on decellularized scaffold

Hematoxylin-eosin staining was performed before and after decellularization of the carotid artery (Fig. 8a, b). As can be seen in Fig. 8b, after decellularization, there were no remaining cells, and a cell-free extracellular matrix was observed. This extracellular matrix was used as a scaffold for VSMCs culture. SEM was used to study the topographical features and morphology of the ECM network composed of elastin and collagen fibers. Fig. 8c, d illustrates the size distribution of matrix fibers ranging from 1 to 10  $\mu\text{m}$  with an average of 6  $\mu\text{m}$ .

After the decellularization step (Fig. 9-a), VSMCs were seeded on the decellularized scaffold (Fig. 9b, c, d) at a density of  $3 \times 10^5$  cells/cm $^2$ , followed by incubation in a humidified atmosphere with 5 % CO<sub>2</sub> for 72 h. Electrical stimulation was initiated approximately 30 min after cell seeding on the decellularized scaffold, using a 1000  $\mu\text{A}$  ( $\pm 1$  V) sinusoidal electrical stimulation at 10 Hz for 20 min every 24 h. After 72 h, the cultured cells on the scaffold were imaged using a scanning electron microscope (Fig. 9-b, c, d). The examples of the stimulated and non-stimulated VSMCs cultured on the decellularized scaffold, have been shown by red arrows in Fig. 9. While Fig. 9b indicates that the non-stimulated individual VSMCs lie in a disordered arrangement (Fig. 9b). However, it can be seen in Fig. 9c,d that the stimulated VSMCs lie on the ECM regularly with the elongated morphology compared with the non-stimulated one. Table 2 and Fig. 10 show the lengths of stimulated and non-stimulated VSMCs which were calculated by the ImageJ software. Based on the results, the average of VSMC length increased from 27.05 micrometers to 47.386 micrometers due to electrical stimulation. The contractile phenotype has a more extended morphology than the synthetic phenotype, so It can be concluded that electrical stimulation can affect the phenotypic differentiation of VSMCs, which is also supported by the previous findings of this study.

## 4. Conclusion

In this research, phenotype switching of VSMCs in response to electrical stimulation was investigated. The stimulated cells exhibited a more elongated morphology and also reduced levels of vimentin, nestin and  $\beta$ -actin expression, compared to the non-stimulated cells. On the other hand, the expression levels of VSMC differentiation markers, namely SMMHC and  $\alpha$ -SMA, increased after electrical stimulation. Therefore, it has been demonstrated in this work that electrical current can direct VSMCs toward a more contractile phenotype. It may be concluded that electrical stimulation can change the phenotype of vascular smooth muscle cells and can be an effective option to prevent the aberrant proliferation of VSMCs and subsequent occlusion of arteries in vascular tissue engineering.

## CRediT authorship contribution statement

Author 1 Author 2 Author 3 Author 9 Conceptualization Methodology / Study design. Author 1 Author 2 Author 9 Formal analysis. Author 1 Author 2 Author 3 Author 8 Author 9 Investigation. Author 1 Author 2

Author 3 Author 4 Author 5 Author 6 Author 7 Author 8 Author 9 Resources. Author 1 Author 2 Author 3 Author 4 Author 5 Author 6 Author 7 Author 8 Author 9 Data Collection. Author 1 Author 2 Author 9 Writing – original draft. Author 1 Author 2 Author 3 Author 8 Author 9 Writing – review and editing. Author 2 Author 3 Supervision.

## Data availability

Data will be made available on request.

## Appendix A. Supporting information

Supplementary data associated with this article can be found in the online version at doi:10.1016/j.tice.2022.101996.

## References

- Amberg, G.C., Navedo, M.F., 2013. Calcium dynamics in vascular smooth muscle. Microcirculation 20 (4), 281–289. <https://doi.org/10.1111/micc.12046>.
- Bacakova, L., Travnickova, M., Filova, E., Matéjka, R., Stepanovska, J., Musilkova, J., Zarubova, J., & Martin Molitor, M. (2018a). The role of vascular smooth muscle cells in the physiology and pathophysiology of blood vessels. In (Ed.), Muscle Cell and Tissue - Current Status of Research Field, Editor:Kunihiro Sakuma, IntechOpen. <https://doi.org/10.5772/intechopen.77115>.
- Bacakova, L., Travnickova, M., Filova, E., Matéjka, R., Stepanovska, J., Musilkova, J., Zarubova, J., & Martin Molitor, M. (2018b). Vascular smooth muscle cells (VSMCs) in blood vessel tissue engineering: the use of differentiated cells or stem cells as VSMC precursors. In (Ed.), Muscle Cell and Tissue - Current Status of Research Field. IntechOpen. <https://doi.org/10.5772/intechopen.77108>.
- Battaglia, R.A., Delic, S., Herrmann, H., Snider, N.T., 2018. Vimentin on the move: new developments in cell migration. F1000Research 7. <https://doi.org/10.12688/f1000research.15967.1> (F1000 Faculty Rev-1796).
- Beamish, J.A., He, P., Kottke-Marchant, K., Marchant, R.E., 2010. Molecular regulation of contractile smooth muscle cell phenotype: implications for vascular tissue engineering. Tissue Eng. Part B, Rev. 16 (5), 467–491. <https://doi.org/10.1089/ten.teb.2009.0630>.
- Catto, V., Farè, S., Freddi, G., Tanzi, M.C., 2014. Vascular tissue engineering: recent advances in small diameter blood vessel regeneration. Int. Sch. Res. Not. 2014, 27. <https://doi.org/10.1155/2014/923030>.
- Chakraborty, R., Chatterjee, P., Dave, J.M., Ostriker, A.C., Greif, D.M., Rzucidlo, E.M., Martin, K.A., 2021. Targeting smooth muscle cell phenotypic switching in vascular disease. JVS-Vasc. Sci. 2, 79–94. <https://doi.org/10.1016/j.jvssc.2021.04.001>.
- Chen, L., DeWispelaere, A., Dastvan, F., Osborne, W.R., Blechner, C., Windhorst, S., Daum, G., 2016. Smooth muscle-alpha actin inhibits vascular smooth muscle cell proliferation and migration by inhibiting Rac1 activity. PLOS One 11 (5), e0155726. <https://doi.org/10.1371/journal.pone.0155726>.
- Chung, B.M., Rotty, J.D., Coulombe, P.A., 2013. Networking galore: intermediate filaments and cell migration. Curr. Opin. Cell Biol. 25 (5), 600–612. <https://doi.org/10.1016/j.ceb.2013.06.008>.
- Coats, S., Flanagan, W.M., Nourse, J., Roberts, J.M., 1996. Requirement of p27Kip1 for restriction point control of the fibroblast cell cycle. Science 272 (5263), 877–880. <https://doi.org/10.1126/science.272.5263.877>.
- Dmello, C., Sawant, S., Alam, H., Gangadaran, P., Tiwari, R., Dongre, H., Rana, N., Barve, S., Costea, D.E., Chaukar, D., Kane, S., Pant, H., Vaidya, M., 2016. Vimentin-mediated regulation of cell motility through modulation of beta4 integrin protein levels in oral tumor derived cells. Int. J. Biochem. Cell Biol. 70, 161–172. <https://doi.org/10.1016/j.biocel.2015.11.015>.
- Gabbiani, G., Schmid, E., Winter, S., Chaponnier, C., de Ckhostonay, C., Vandekerckhove, J., Weber, K., Franke, W.W., 1981. Vascular smooth muscle cells differ from other smooth muscle cells: predominance of vimentin filaments and a specific alpha-type actin. Proc. Natl. Acad. Sci. USA 78 (1), 298–302. <https://doi.org/10.1073/pnas.78.1.298>.
- Gerthoffer, W.T., 2007. Mechanisms of vascular smooth muscle cell migration. Circ. Res. 100 (5), 607–621. <https://doi.org/10.1161/01.RES.0000258492.96097.47>.
- Grosskreutz, C.L., Anand-Apte, B., Dupláa, C., Quinn, T.P., Terman, B.I., Zetter, B., D'Amore, P.A., 1999. Vascular endothelial growth factor-induced migration of vascular smooth muscle cells in vitro. Microvasc. Res. 58 (2), 128–136. <https://doi.org/10.1006/mvre.1999.2171>.
- Halayko, A.J., Salari, H., MA, X., Stephens, N.L., 1996. Markers of airway smooth muscle cell phenotype. Am. J. Physiol. 270 (6 Pt 1), L1040–L1051. <https://doi.org/10.1152/ajplung.1996.270.6.L1040>.
- House, S.J., Potier, M., Bisailon, J., Singer, H.A., Trebak, M., 2008. The non-excitable smooth muscle: calcium signaling and phenotypic switching during vascular disease. Pflug. Arch.: Eur. J. Physiol. 456 (5), 769–785. <https://doi.org/10.1007/s00424-008-0491-8>.
- Hu, D., Yin, C., Luo, S., Habenicht, A., Mohanta, S.K., 2019. Vascular smooth muscle cells contribute to atherosclerosis immunity. Front. Immunol. 10, 1101. <https://doi.org/10.3389/fimmu.2019.01101>.
- Huang, S.L., Kee, P.H., Kim, H., Moody, M.R., Chrzanowski, S.M., Macdonald, R.C., McPherson, D.D., 2009. Nitric oxide-loaded echogenic liposomes for nitric oxide

